Research Article Vol. 14, No. 6 / 1 Jun 2023 / Biomedical Optics Express 2955
Biomedical Optics EXPRESS

Spatial frequency domain imaging for the assessment of scleroderma skin involvement

ANAHITA PILVAR,[1] AAROHI M. MEHENDALE,[2] KAVON KARROBI,[2] FATIMA EL-ADILI,[3,4] ANDREEA BUJOR,[3,4] AND DARREN ROBLYER[1,2,*]

[1]Department of Electrical and Computer Engineering, Boston University, Boston, MA 02215, USA
[2]Department of Biomedical Engineering, Boston University, Boston, MA 02215, USA
[3]Division of Rheumatology, Boston University Chobanian & Avedisian School of Medicine, Boston, MA 02118, USA
[4]Arthritis and Autoimmune Diseases Center, Boston University, Boston, MA 02118, USA
*roblyer@bu.edu

Abstract: Systemic sclerosis (SSc) is an autoimmune disease characterized by the widespread deposition of excess collagen in the skin and internal organs, as well as vascular dysfunction. The current standard of care technique used to quantify the extent of skin fibrosis in SSc patients is the modified Rodnan skin score (mRSS), which is an assessment of skin thickness based on clinical palpation. Despite being considered the gold standard, mRSS testing requires a trained physician and suffers from high inter-observer variability. In this study, we evaluated the use of spatial frequency domain imaging (SFDI) as a more quantitative and reliable method for assessing skin fibrosis in SSc patients. SFDI is a wide-field and non-contact imaging technique that utilizes spatially modulated light to generate a map of optical properties in biological tissue. The SFDI data were collected at six measurement sites (left and right forearms, hands, and fingers) of eight control subjects and ten SSc patients. mRSS were assessed by a physician, and skin biopsies were collected from subject's forearms and used to assess for markers of skin fibrosis. Our results indicate that SFDI is sensitive to skin changes even at an early stage, as we found a significant difference in the measured optical scattering (μ_s') between healthy controls and SSc patients with a local mRSS score of zero (no appreciable skin fibrosis by gold standard). Furthermore, we found a strong correlation between the diffuse reflectance (R_d) at a spatial frequency of 0.2 mm^{-1} and the total mRSS between all subjects (Spearman correlation coefficient = -0.73, p-value < 0.0028), as well as high correlation with histology results. The healthy volunteer results show excellent inter- and intra-observer reliability (ICC > 0.8). Our results suggest that the measurement of tissue μ_s' and R_d at specific spatial frequencies and wavelengths can provide an objective and quantitative assessment of skin involvement in SSc patients, which could greatly improve the accuracy and efficiency of monitoring disease progression and evaluating drug efficacy.

1. Introduction

Systemic sclerosis (SSc), or scleroderma, is an autoimmune disorder characterized by fibrosis of the skin and internal organs [1]. SSc is a rare disease with the prevalence of 3.8 to 50 individuals per 100,000 in the world and incidence of 0.77 to 5.6 individuals per 100,000 each year [2,3]. It is more common in females than males (approximately 80% of the diagnosed patients are women) [2]. SSc is typically diagnosed between the age of 30 and 50 with early symptoms such as fatigue, puffy hands with exaggerated response to cold (Raynaud's phenomenon), and joint pain, followed by tightening of the skin [4]. Based on the extent of skin involvement, SSc is classified into two subgroups: diffuse SSc (dcSSc, with skin thickening proximal to elbows and knees) and limited SSc (lcSSc, skin thickening distal to elbows and knees) [1]. Although in rare cases SSc patients develop internal organ complications, autoimmunity and Raynaud's, in the

#489609 https://doi.org/10.1364/BOE.489609
Journal © 2023 Received 10 Mar 2023; revised 11 May 2023; accepted 11 May 2023; published 25 May 2023

Biomedical Optics EXPRESS

absence of obvious skin involvement ("sine scleroderma"), skin thickening caused by excess collagen production remains one of the most common manifestations in SSc [1,4,5]. Accurate quantification of skin fibrosis in scleroderma is of vital importance, as it can provide important clues about the severity of disease, survival and response to therapy [6,7]

The current standard of care for evaluation of the extent of skin involvement in SSc patients is the modified Rodnan Skin Score (mRSS, integer scale 0-3), which is an estimate of skin thickness by clinical palpation [8]. mRSS = 0 refers to normal skin with no appreciable skin thickening and mRSS = 3 refers to the most severe skin thickening. The mRSS is used as the primary outcome measure or a key secondary outcome measure in clinical trials; however it has several limitations. mRSS is a semi-quantitative assessment of skin that requires a well-trained rheumatologist. The subjective assessment often results in large inter-observer variability [9,10]. Other conditions such as edema and atrophy are confounding factors that may affect the mRSS assessment [8]. Additionally, sensitivity to longitudinal changes in SSc skin condition is an important aspect of SSc evaluation specially in clinical trials which cannot always be achieved by mRSS assessment [11]. A new and improved method for rapid, objective, and reproducible evaluation of skin fibrosis is an unmet need both in the clinic and for clinical trials.

Several studies have employed different modalities such as ultrasound, optical coherence tomography (OCT), and durometry to improve the assessment of skin in SSc patients [12–15]. Ultrasound showed significantly increased skin thickness in SSc patients compared to healthy controls [12]. OCT showed a correlation between the measured optical density (OD) and mRSS [14]. Durometry showed a correlation between the skin hardness and mRSS in SSc patients [15]. However, none has been adapted by clinicians or clinical trials as a substitute for mRSS for reasons such as high level of required training, small measurement region, low repeatability, complex postprocessing and difficulties in result interpretation. The ideal method for SSc assessment needs to be objective, consistent and repeatable, easy to use, sensitive to small variations, provide large field of view to avoid sampling bias and have a better ability to resolve small differences compare to mRSS.

Spatial frequency domain imaging (SFDI) is a non-contact optical technique for non-invasive assessment of tissue optical properties. The measured optical properties provide functional and structural information about the tissue [16]. SFDI has been widely used over the past decade for several dermatology applications and skin characterization [17–20]. Depending on the measurement parameters (such as wavelength and spatial frequency), SFDI has the depth resolution of submillimeter to few millimeters from the tissue surface, making the technique suitable to assess the dermal layer of skin, where fibrosis is presented in SSc [5,14]. Here for the first time, we test the feasibility of SFDI as a potential imaging tool for SSc skin assessment compared to mRSS (clinical gold standard) and histopathology results (reliable indicators of disease progression).

2. Materials and methods

2.1. Subject eligibility and enrollment

The study was conducted in compliance with an approved institutional review board protocol, applicable regulatory requirements, and BMC/BU Medical Campus Human Research Protection policies and procedures (protocol number 38234). Subjects were informed about the study and provided informed consent prior to the experiment at the time of regularly scheduled clinic visits. Patients with different degrees of skin involvement were enrolled in the study. Control subjects had no skin disease and were chosen to cover the age range and skin tone variability of the enrolled patients. All scleroderma patients and healthy controls underwent SFDI measurements, mRSS assessments, and skin biopsies. An additional healthy volunteer study was conducted for inter- and intra-observer variability test with the SFDI system on 10 healthy subjects (protocol number 4698).

Biomedical Optics EXPRESS

2.2. Spatial frequency domain imaging (SFDI) technique

Spatial Frequency Domain Imaging (SFDI) is a non-contact diffuse optical imaging modality for non-invasive measurements of tissue optical properties, namely absorption (μ_a) and reduced scattering (μ_s'). SFDI provides wavelength dependent maps of tissue optical properties over a wide field of view on a pixel-by-pixel basis. Detailed descriptions of SFDI instrumentation and data analysis are provided elsewhere [16,21]. Briefly, sinusoidal spatial patterns of light are projected on a sample using a digital micro-mirror device (DMD), and the remitted light is captured by a camera (Figure 1(A)). A flowchart of SFDI data acquisition and processing is provided in Figure 1(B). The patterns are projected at multiple wavelengths and spatial frequencies. At least two spatial frequencies are required for quantification of μ_a and μ_s'. At each spatial frequency, three sinusoidal images at three different spatial phases (0°, 120° and 240°) are projected. The captured images are demodulated using the following demodulation method (Eq. (1)):

$$I = \frac{\sqrt{2}}{3}\sqrt{(I_1 - I_2)^2 + (I_2 - I_3)^2 + (I_1 - I_3)^2} \tag{1}$$

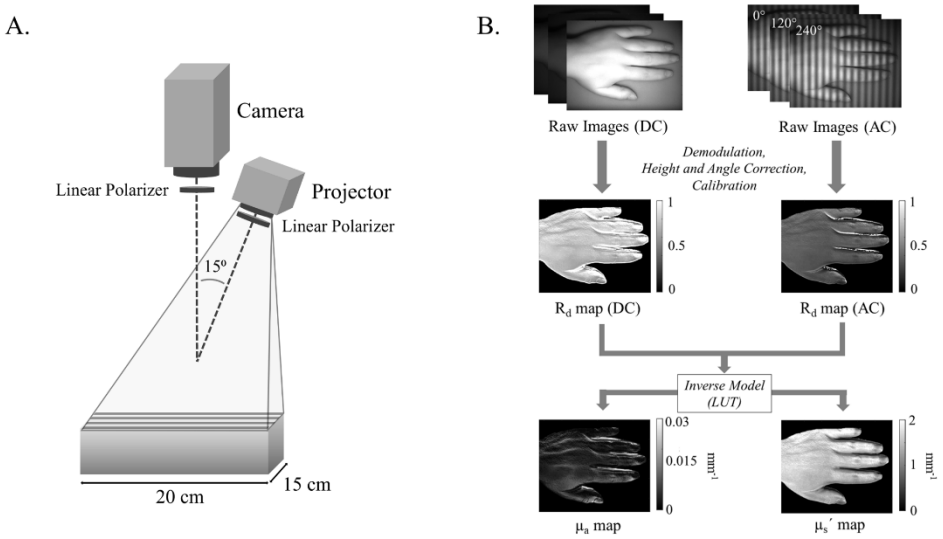

Fig. 1. A) Schematic diagram of a SFDI system. The illumination source is a set of VIS-NIR LEDs. The illumination source combined with a DMD is labeled as projector in this diagram. Two crossed polarized linear polarizers are placed in the illumination and detection path to avoid specular reflection. B) SFDI data acquisition and processing flowchart. Top row represents the captured raw images at DC and AC at 851 nm. The raw AC images are the three phases captured at a spatial frequency of 0.1 mm^{-1}. Three DC images are taken at different intensity counts, demodulated and used for background correction. Raw AC images are demodulated, corrected for height and angle variability, and calibrated. The middle row represents the calibrated diffuse reflectance (R_d) maps at DC and AC. The R_d maps are converted into optical property maps (μ_a and μ_s') using a LUT inverse model.

The resulting demodulated image (I) at each spatial frequency is then calibrated using a calibration phantom with known and stable optical properties to account for any instrument response and produce an image of calibrated diffuse reflectance (R_d). The calibrated R_d images at two spatial frequencies are then converted to a unique set of μ_a and μ_s' using a Monte Carlo based lookup table (LUT) inversion algorithm. A homogeneous and semi-infinite model was used to process the data [21,22].

Biomedical Optics EXPRESS

In this study, a research SFDI system from Modulim (Reflect RS; Modulim Inc. Irvine, CA) was utilized to perform all the SFDI measurements. The Modulim system utilizes wavelengths from the visible to the NIR. The field of view (FOV) of the SFDI images is 15 × 20 cm. The remitted light from the tissue is collected by a CCD camera. To account for height and angle variabilities within the sample FOV compared to the calibration phantom measurement, we performed height and angle correction in this study on the demodulated images using a previously developed height and angle correction algorithm [23].

2.3. Imaging procedure

SFDI measurements were taken at three body locations: finger, dorsal surface of the hand, and dorsal surface of the forearm. The three locations were imaged on both left and right sides of the body. Hand and finger measurements were taken at the same time since the SFDI field of view covers the entire hand area. Forearm measurements were taken separately. The subjects were asked to be seated on a chair and place their hand or forearm under the SFDI instrument. Measurements were taken at 8 wavelengths (471, 526, 591, 621, 691, 731, 811, and 851 nm) and 8 spatial frequencies (DC, 0.05, 0.1, 0.15, 0.2, 0.3, 0.4 and 0.5 mm^{-1}). The profilometry measurements for height and angle correction were performed at f_x= 0.05 mm^{-1} and wavelength = 691 nm. Two repeat measurements were performed for each location. Each measurement took 2 minutes and total measurement time for each subject was less than 15 minutes.

2.4. Skin thickness score assessment (mRSS) and histopathology

mRSS assessments were performed by an expert rheumatologist (A.B.) for each subject. mRSS was determined at 17 locations across the body (fingers, hands, forearms, upper arms, face, interior chest, abdomen, thighs, legs, and feet) with the standard 0 (normal), 1 (mildly thickened), 2 (moderately thickened), and 3 (severely thickened) scale, as previously described [8]. The total mRSS for each subject was calculated by summing the mRSS across all location sites.

Skin biopsies: After SFDI measurements and mRSS assessment, biopsies were obtained by A.B. from the dorsal mid forearm of SSc patients and healthy controls during the same visit and after informed consent. Subjects were given local anesthetic at the site of the biopsy, and one 3 mm circular skin sample was obtained using a dermal biopsy punch under sterile conditions. Steristrips and tegaderm were then placed at the biopsy site, and the sample was coded. Specimens were fixed with 10% buffered formalin and embedded in paraffin for immunohistochemistry. Trichrome staining of paraffin-embedded skin sections followed by semi-quantitative assessment of collagen was performed according to manufacturer's protocol and as previously described, using a commercially available kit (HT15, Sigma-Aldrich, St. Louis, MA, USA) [24]. Semi-quantitative assessment of dermal fibroblast activation was assessed by calculating the myofibroblasts score using immunohistochemistry for alpha smooth muscle actin (ASMA) according to a published protocol [24].

2.5. Inter- and intra-observer reliability study

Inter- and intra-observer reliability studies were conducted to assess the construct validity and reliability (OMERACT filter of "truth") and the test-retest reliability (OMERACT filter of "discrimination") respectively. Nine healthy controls with mean age 31.8 ± 17.3 (range 23-76) were measured for the inter-observer reliability study [25]. SFDI measurements were performed on subjects' right hand, fingers, and forearm. Measurements were taken consecutively by two operators during the same imaging session. Subjects removed their hand and forearm and replaced them under the SFDI system between each measurement. The operators were not present in the room during the other operator's measurement session.

Biomedical Optics EXPRESS

10 healthy controls with mean age 31.5 ± 16.4 (range 23-76) were measured for the intra-observer reliability study. SFDI measurements of the subjects' right hand, fingers and forearm were taken by the same operator during the same imaging session, with a 5-minute break between measurements. Subjects removed and replaced their hand and forearm during this break.

The intraclass correlation coefficient (ICC) was calculated to estimate the inter- and intra-observer reliability of SFDI measurements. A one-way random effect model was used based on the design of the experiment [26]. ICC > 0.8 was considered as excellent agreement according to the scale from Altman [27]. In addition, a Bland-Altman analysis was performed, and limits of agreement (LoA) were calculated based on 95% confidence intervals [27].

2.6. Data analysis

2.6.1. ROI selection

Regions of Interest (ROIs) were selected from the SFDI maps for comparison of SFDI derived parameters and their correlation with clinical measurements. The mean values from the selected ROIs were used as representative values for each anatomical site. The ROIs were selected to cover maximum area of the measurement site to ensure that all the spatial information was taken into consideration. An example ROI selection is shown in Figure S1. All ROIs were rectangular in shape and selected on MATLAB (R2021b, The Mathworks Inc., Natick, MA). On the dorsal forearm, a rectangular ROI of dimensions 800 × 300 pixels (approx. 4.3 × 11.5 cm), aligned along the forearm was used. On hand, a square ROI of dimension 300 × 300 pixels (approx. 4.3 × 4.3 cm) centered on the dorsal palm between the wrist and knuckles was used. On fingers, five small rectangles, each of dimension 100 × 25 pixels (1.44 × 0.36 cm) were selected between the metacarpophalangeal joint (MCP) and the proximal interphalangeal joint (PIP) on the dorsal side for each finger and were averaged to provide one representative value for finger location.

2.6.2. Statistical analysis

Wilcoxon rank sum tests were used to investigate potential statistical differences in SFDI-derived parameters between groups of healthy controls and SSc patients, and Wilcoxon signed rank tests were used for differences between anatomical regions from SSc subjects with mRSS = 0 and regions with mRSS > 0. To evaluate the correlation between the SFDI parameters and mRSS and histopathology metrics, Spearman rank correlation was used to determine the coefficient of correlation. A p-value < 0.05 was considered statistically significant. All data were analyzed with MATLAB.

3. Results

3.1. Subject enrollment

Data from 10 scleroderma patients (1 male and 9 female) and 8 healthy controls (1 male and 7 female) were included in this analysis. Scleroderma patients had an average age of 50 ± 16 (26-74 range) and the control group had an average age of 43 ± 13 (27-63 range). The local mRSS for SSc patients ranged from zero (no skin thickening) to 3 (severe skin thickening). Subjects self-reported their race and ethnicity as Black, Hispanic, and/or White. The summary of subject information is shown in Table 1.

3.2. SFDI results

Imaging data was processed and calibrated R_d values were determined at all measured spatial frequencies and wavelengths. The spatial frequency pair of DC and 0.1 mm^{-1} was used for all optical property calculations.

Figure 2 shows the white light image of the hand of a representative healthy control and a SSc patient (mRSS of 1 in the hand location, and the total mRSS of 24) with similar skin tones. The

Biomedical Optics EXPRESS

Table 1. Epidemiological and clinical summary of enrolled subjects.

	SSc	Healthy Controls
Total	N = 10	N = 8
Sex		
Male	N = 1	N = 1
Female	N = 9	N = 7
Race/Ethnicity		
Black	N = 3	N = 5
Hispanic	N = 2	N = 1
White	N = 5	N = 2
Skin status		
mRSS = 0	N = 3	N/A
mRSS > 0	N = 7	N/A
Mean Age	50 ± 16 (y.o.)	43 ± 13 (y.o.)

bottom row demonstrates the μ_s' map at 851 nm of the hand location for the same subjects. The μ_s' maps show that there is a notable decrease in reduced scattering in the patient with scleroderma compared to the healthy subject, a difference that cannot be quantitatively discerned from the white light data.

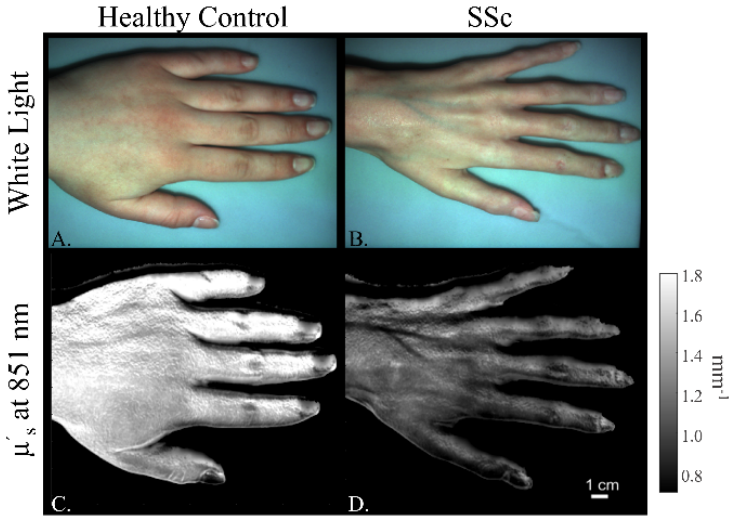

Fig. 2. Top row: White light images of left hand from a representative healthy control and a scleroderma patient with mRSS = 1 at the hand. Both subjects self-identified as white. Bottom row: μ_s' map of the same location at 851 nm. The scleroderma patient had a lower μ_s' compared to the healthy subject.

The average optical properties inside selected ROIs (Figure S1) were then calculated at each measurement site and the spectral data were plotted for both patients and controls. Figure 3(A) shows the μ_a spectra from hand, finger, and arm location of SSc patients and control subjects. There was no significant difference in the measured μ_a between SSc patients and healthy controls at any of the measurement wavelengths (Wilcoxon rank sum test, p values ranging from 0.84-0.94). Conversely, there is an obvious separation between scleroderma patients and healthy control

Biomedical Optics EXPRESS

subjects in μ_s' spectra, especially at the longest wavelength of 851 nm (Figure 3(B)). Spectra from individual anatomical sites are shown in Figure S2.

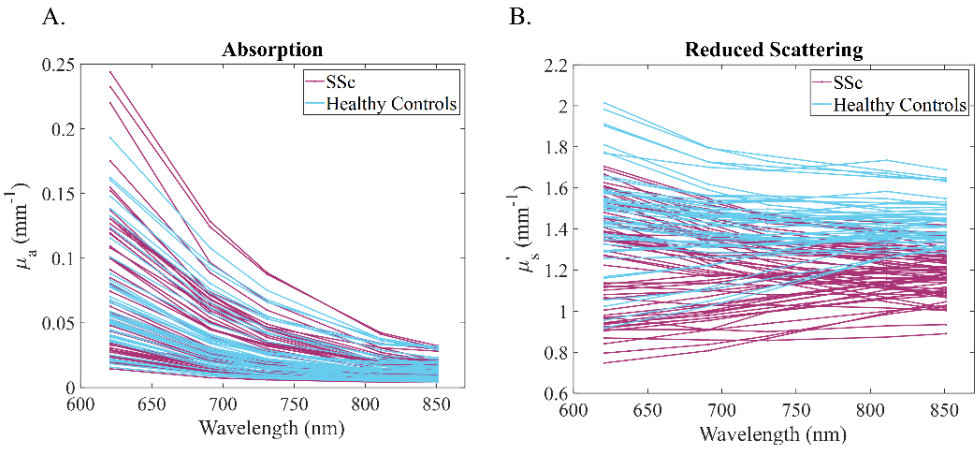

Fig. 3. A. Absorption and B. reduced scattering coefficient spectra from all measurement locations of SSc subjects (magenta) and healthy controls (blue). Each line represents a different anatomic location. A strong separation between SSc and healthy controls was observed for μ_s' at 851 nm. In the interest of conciseness, only the longest five wavelengths have been included in the spectra.

It has been previously observed that subject's skin tone affects both μ_a and μ_s' spectra, especially at shorter wavelengths where melanin has strong absorption characteristics [28]. In the μ_a spectra, subjects with darker skin tone exhibited higher absorption values (data not shown), likely due to high melanin content in the epidermis. It is of note that for the μ_s' spectra, the commonly observed power law spectral behavior of reduced scattering in tissue did not always hold for subjects with darker skin tone. Rather, μ_s' was observed to increase with wavelength rather than decrease for those with darker skin tones. This phenomenon has been previously observed in a prior SFDI study, especially in subjects with darker skin (i.e. higher Fitzpatrick skin scores) [29]. That study suggested that a wavelength-dependent partial volume effect due to the strong absorption of melanin may be responsible for this observation, and the use of longer wavelengths may be helpful when comparing subjects with different skin tones because of the reduced influence of melanin. Similarly, here the μ_s' at long NIR wavelengths such as 851 nm appeared to be less sensitive to skin tone and could better distinguish SSc patients from controls.

The performance of μ_s' in discriminating SSc subjects from healthy controls across race and ethnicity was further evaluated at two different wavelengths (691 nm and 851 nm). Figure 4 clearly demonstrates the better performance of the longer wavelength at 851 nm in distinguishing subjects with SSc from healthy controls compared to the shorter 691 nm wavelength, particularly in Black and Hispanic subjects. Statistically, lower p-values were associated with the difference between the μ_s' values of SSc and Healthy Controls for White and Black Subjects as wavelength increased from 691 nm to 851 nm (Wilcoxon rank sum test, White: $p = 2.8e\text{-}4$ (691 nm) and $p = 9.0e\text{-}6$ (851 nm), Black: $p = 4.8e\text{-}8$ (691 nm) and $p = 3.9e\text{-}10$ (851 nm)). The p-values for Hispanic Subjects remained the same across wavelengths (Wilcoxon rank sum test, $p = 5.3e\text{-}6$).

3.3. Correlation between imaging parameters and mRSS

To evaluate the differences between healthy controls and SSc patients, the average value of μ_s' was calculated at each SFDI measurement site (each subject had six sites from the three body locations measured: left and right hands, fingers, and forearms). Although there was a difference between

Biomedical Optics EXPRESS

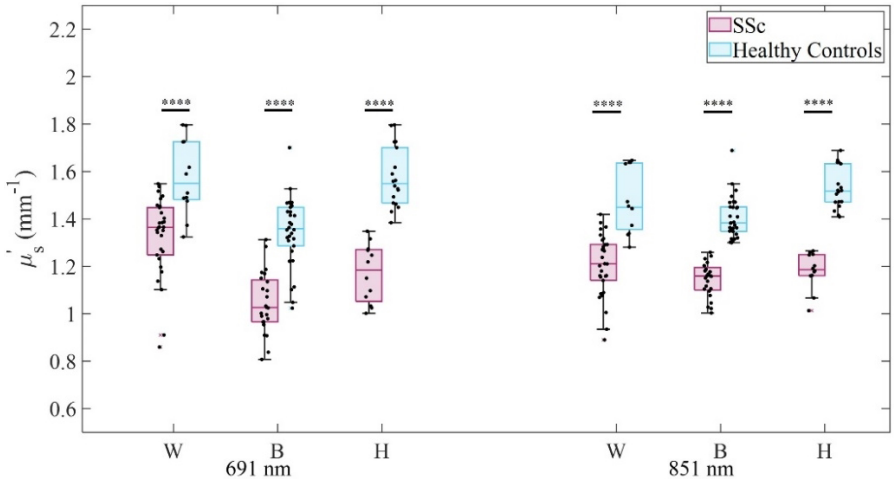

Fig. 4. Comparing the performance of μ_s' at an example shorter (691 nm) and longer (851 nm) NIR wavelength in differentiating SSc from healthy controls for subjects with different race/ethnicity. W: White, B: Black, H: Hispanic. Box plots represent 25th and 75th percentiles, median as a line inside the box, and minimum and maximum values as whiskers. Asterisks indicate level of significance, ****$p < 0.0001$.

average age of the healthy controls and SSc patients, no statistically significant correlation was found between age and μ_s'. Figure 5(A) illustrates a boxplot that compares the μ_s' at 851 nm of healthy controls at all sites to the μ_s' of SSc patients. Healthy controls had a statistically significant higher μ_s' compared to the SSc subjects (Wilcoxon rank sum test, p-value < 0.0001). Differences between healthy controls and patients for individual anatomical sites are shown in Figure S3. In Figure 5(B), the results of the SSc patients were separated into two subgroups: μ_s' from the locations with no evident skin fibrosis (mRSS = 0), and μ_s' from the locations with any level of skin fibrosis (mRSS > 0). The difference between the measured μ_s' of healthy controls and SSc patients in the locations where mRSS = 0 was statistically significant (Wilcoxon rank sum test, p-value < 0.0001). Furthermore, there is a significant difference between the measured μ_s' of locations with mRSS = 0 in the patient population and locations with any level of skin fibrosis (mRSS > 0) (Wilcoxon signed rank test, p-value = 0.01).

Figure 6(A) shows the correlation between the local μ_s' and local mRSS of subjects with SSc, with each plotted data point representing an individual subject. The local μ_s' was calculated by summing the μ_s' at all six measurement sites (left and right hands, fingers, and forearms), and the local mRSS was calculated as the sum of the mRSS from the same six sites. The correlation between the local μ_s' and the total mRSS from all 17 locations where mRSS was assessed is shown in Figure S4. While there was a trend, there was not a significant correlation between local μ_s' and local mRSS (Spearman correlation coefficient = -0.57, p = 0.083). We did find however that there was a statistically significant correlation between the local R_d at $f_x = 0.2$ mm^{-1} and the local mRSS as shown in Figure 6(B) (Spearman correlation coefficient = -0.77, p = 0.0089). These results suggest that while μ_s' at 851 nm may be an excellent SFDI metric to differentiate healthy subjects from SSc patients, as well as SSc patients with preclinical skin involvement from those with evident skin fibrosis (Figure 5), R_d at 0.2 mm^{-1} better correlates with the mRSS for subjects with clinical skin involvement (Figure 6(B)).

Biomedical Optics EXPRESS

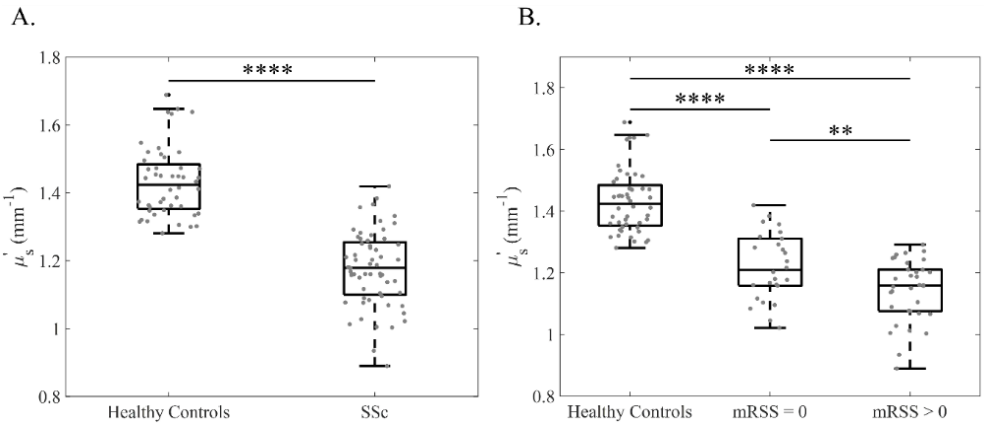

Fig. 5. The boxplots of measured μ_s' at 851 nm for all measurement sites. A) μ_s' difference between healthy controls and SSc patient. B) μ_s' difference between healthy controls, SSc patient at locations where there is no skin fibrosis (mRSS = 0), and SSc patients at measurement sites with skin fibrosis (mRSS > 0). Box plots represent 25th and 75th percentiles, median as a line inside the box, and minimum and maximum values as whiskers. Asterisks indicate level of significance, ****$p < 0.0001$, **$p \leq 0.01$.

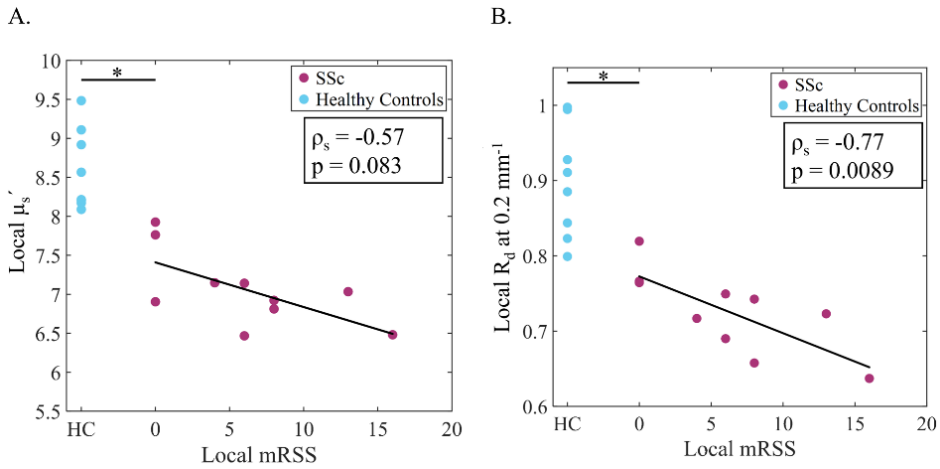

Fig. 6. A) Correlation between the local μ_s' at 851 nm and local mRSS of subjects with SSc (Spearman correlation coefficient = -0.57, p = 0.083). B) Correlation between local R_d at $f_x = 0.2\ mm^{-1}$ and local mRSS of subjects with SSc (Spearman correlation coefficient = -0.77, p = 0.0089). The local values were calculated by adding the SFDI parameter from all measurement sites and mRSS from the same sites. Also shown are significant differences (Wilcoxon rank sum test, *$p < 0.05$) of the local μ_s' at 851 nm and local R_d at $f_x = 0.2\ mm^{-1}$ between subjects with SSc and Healthy Controls.

3.4. Correlation between diffuse reflectance and histology scores

Activation of local dermal fibroblasts into ASMA-expressing myofibroblasts with excessive collagen production is a hallmark process during disease progression in SSc [30]. Previously, studies have shown a correlation between an increase in myofibroblasts and mRSS [24]. We next evaluated correlations of fibroblast activation and total collagen content with local SFDI score in SSc and HC biopsies. Semi-quantitative assessment of dermal fibroblast activation

Biomedical Optics EXPRESS

was assessed by calculating the myofibroblasts score using immunohistochemistry for alpha smooth muscle actin (ASMA) as previously described [24]. The biopsy specimens were taken from subjects' forearms and the SFDI data shown was acquired at the matching biopsy location. Figure 7 shows the correlation between the histology results and the R_d at $f_x = 0.2$ mm^{-1} and 851 nm. Figure 7(A) shows an excellent correlation between average R_d and myofibroblast score between all subjects (Spearman correlation coefficient = -0.88, p-value < 0.0001). Similarly, histological quantification of collagen content using Trichrome staining score in Figure 7(B) shows a strong correlation with R_d (Spearman correlation coefficient = -0.73, p-value = 0.0028) [24]. The negative correlation between Trichrome score and R_d suggests that excess collagen in SSc patients result in lower reflectance of light from superficial layers.

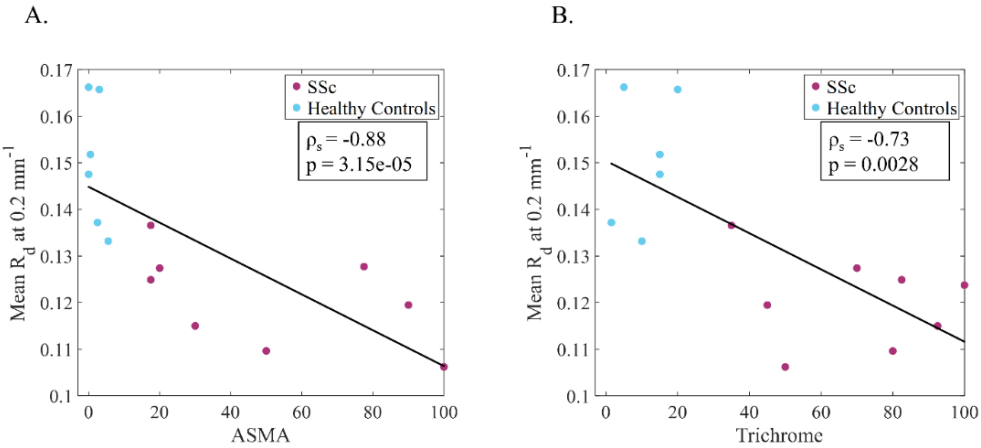

Fig. 7. Correlation between the average R_d ($f_x = 0.2$ mm^{-1}, wavelength = 851 nm) at arm location and histology results of biopsy sample taken from the same arm. A) Correlation between R_d and ASMA (Spearman correlation coefficient = -0.88, p-value < 0.0001). B) Correlation between R_d and Trichrome staining (Spearman correlation coefficient = -0.73, p-value < 0.0028).

3.5. Inter- and intra-observer reliability results

Inter- and intra-observer reliability was assessed based on μ_s' values at 851 nm, calculated from the spatial frequency pair of DC and 0.1 mm^{-1}. ROIs of the same size as in the clinical measurement were chosen on the right forearm, hand, and fingers. ROIs were selected in the same relative anatomic location for each subject between repeated tests. As shown in Table 2, ICC calculations indicate that SFDI measurements have excellent inter- and intra-observer reliability, with ICC ranges of 0.82-0.99 and 0.96-0.99 respectively. Comparatively, mRSS has an inter-observer ICC of 0.63-0.68 and intra-observer ICC of 0.74-0.76 [9,10]. Bland-Altman analysis and calculated limits of agreement are shown in Figure S5.

3.6. Tissue imaging depth

Tissue imaging depth is likely a key factor related to accurate assessment of fibrosis in SSc. Prior work has shown that sub-millimeter to millimeter depth sensitivity is relevant to skin fibrosis caused by scleroderma [14,31]. Tissue imaging depth depends on the wavelength of light and the optical properties of the tissue sample. Generally, lower spatial frequencies penetrate deeper into tissue compared to higher spatial frequencies at a given wavelength. The penetration depth of illuminated light at each spatial frequency was calculated using a previously established penetration depth estimation method for SFDI [32]. We calculated the estimated

Biomedical Optics EXPRESS

Table 2. Intraclass correlation coefficients (ICC) for inter-and intra-observer measurements at each measurement location. A one-way random effect model was used to compute ICCs.

Measurement Location	Inter-observer Measurement ICC	Intra-observer Measurement ICC
Arm	0.82	0.97
Hand	0.85	0.96
Finger	0.99	0.99

median penetration depth assuming average optical properties measured at the hand and forearm at 851 nm. The median penetration depth ranged from 0.23 mm at the highest spatial frequency ($f_x = 0.5\ mm^{-1}$) to 1.31 mm at the lowest spatial frequency (DC). The fact that R_d at $f_x = 0.2$ mm^{-1} had the best correlation with local mRSS as well as to histology suggests this spatial frequency is well matched to tissue depths related to fibrosis and/or tissue remodeling in SSc.

The calculation of tissue optical properties, including μ_s', requires a combination of at least two different spatial frequencies, complicating the assessment of imaging depth. In this work, the spatial frequency pair of DC and 0.1 mm^{-1} was used for all optical property calculations, although all combinations were evaluated. The combination of a high spatial frequency paired with a low spatial frequency (e.g., DC) is known to lead to a partial volume effect when measuring layered media such as skin [22]. This means that measurements with different imaging depths are combined during processing. In some cases, this partial volume effect may reduce sensitivity to changes occurring at specific depths in tissue [33].

4. Discussion

Here we have demonstrated for the first time the validity of using SFDI to quantify the extent of skin fibrosis in patients with scleroderma. We conducted a study of healthy controls and SSc patients with varying levels of disease severity and compared the performance of SFDI-derived parameters to mRSS as well as histopathology results. mRSS, which is the current gold standard for SSc skin assessment, suffers from several limitations such as subjectivity, a high level of skill requirement, and large inter-observer variability. SFDI, on the other hand, is an objective measure of skin condition that is fast, easy to perform and requires mild operator training.

The SFDI metric that best differentiated between healthy subjects and SSc patients was the μ_s' parameter measured at 851 nm. We showed that measurements of μ_s' at 851 nm were less affected by skin tone compared to shorter wavelengths. μ_s' at 851 nm was also capable of differentiating between healthy subjects and SSc patients that had no clinical signs of skin involvement, as shown with the statistically significant difference between healthy controls and patients with mRSS = 0. This is particularly important at early stages of the diseases in which the mRSS lacks sufficient sensitivity to identify early-phase skin changes.

While μ_s' at 851 nm was excellent at discriminating early disease from healthy skin, the R_d parameter measured at $f_x = 0.2\ mm^{-1}$ demonstrated the best correlation with mRSS and histology results within SSc patients. The Spearman correlation coefficient between the measured R_d (0.2 mm^{-1}) and mRSS score was −0.77. This result outperforms the correlation between mRSS and relative optical density (OD) measured with OCT (correlation coefficient = 0.7) [14]. Our correlation was also stronger than that found using durometry (correlation coefficient = 0.69) [15].

Comparison of μ_s' with mRSS and R_d with skin biopsy results showed a decrease in optical scattering and diffuse reflectance with increases in mRSS, myofibroblast, and Trichrome scores. μ_s' is a marker of tissue morphology and structure. It provides information about optical scattering caused by factors such as the makeup of the extracellular matrix, cellular density, and spatial

Biomedical Optics EXPRESS

variations in refractive index caused by tissue microstructure [34]. The observed reduction in μ_s' with increased mRSS may be due to changes in collagen fiber orientation and fiber density in SSc subjects. Other changes such as reductions or displacements of lipids and loss of tissue differentiation between epidermal and dermal layer [14] may also contribute to the decrease in μ_s' with mRSS. Similarly, R_d measured at 0.2 mm^{-1} is highly influenced by tissue optical scattering [35]. Compared to μ_s', R_d at 0.2 mm^{-1} is more sensitive to superficial layers of skin as it does not utilize planar (DC) measurements, which have a deeper penetration [32]. This sensitivity to superficial layers of skin may be the reason for the better observed correlation of R_d with mRSS, especially at later stages of SSc [8]. R_d at 0.2 mm^{-1} may be a sufficient metric for evaluation of SSc skin involvement. The measurement of R_d at 0.2 mm^{-1} avoids the partial volume mismatch associated with SFDI measurements, which require a combination of measurements taken at different spatial frequencies, each of which has a different depth penetration [32]. The simplicity of this measurement, which does not require extraction of optical properties or an inverse model, and thus is both different and simpler than the SFDI method, could lead to a faster and more compact SSc analyzing device.

Our SFDI results on healthy subjects show low inter- and intra-observer variability (ICC ranges of 0.82-0.99 for inter- and 0.96-0.99 for intra-observer reliability). This is as good or better than ICC values reported for durometry [15] and OCT [14].

Our results strongly support the use of SFDI for SSc skin evaluation as an objective method to assess extent of disease and response to therapy. However, the current technique suffers from some limitations. For example, due to the difficulties in body positioning under the device, we only acquired SFDI measurements from body sites where positioning was easy and comfortable for the subjects. Hence, we did not assess the performance of SFDI at all the 17 anatomic regions assessed for mRSS. In the future, a more compact or hand-held device would assist in validating SFDI for skin evaluation over the entire body. Another limitation is the small sample size with only 10 SSc and 8 HC tested. Since a statistically significant outcome in a small sample does not always reflect a real effect, larger studies are required to fully validate SFDI in SSc [36].

5. Conclusion

In summary, we validate the performance of SFDI measurements for scleroderma skin evaluation compared to the gold standard mRSS and histology markers. We identified μ_s' as the best SFDI metric to differentiate between SSc patients and healthy controls, even in patients with no clinical skin involvement at the measurement locations. R_d at the spatial frequency 0.2 mm^{-1} was identified as the metric that best correlated with mRSS, myofibroblast score, and ASMA score within SSc subjects. Despite the limitations, our results suggest that SFDI is a promising objective alternative to the current standard of care for SSc skin evaluation. The non-contact, non-invasive, wide-field, and quantitative nature of the technique, as well as the high reliability and repeatability of the measurements, make SFDI a potentially powerful tool for SSc skin assessment.

Funding. National Institute of Biomedical Imaging and Bioengineering (1R21EB030197); Scleroderma Clinical Trials Consortium (SCTC); Boston University Affinity Research Collaborative (ARC): Connecting Tissues and Investigators (Fibrosis in Pathology).

Acknowledgements:. The authors are grateful to the participants who took part in the study. We wish to thank the study coordinators involved in the study and the clinical staff for assisting with the recruitment of participants.

Disclosures. A.P., A.M., K.K., A.B. and D.R. have submitted a patent disclosure related to the technology in this publication.

Data availability. All relevant code, data, and materials are available from the authors upon reasonable request. Correspondence and requests should be addressed to the corresponding authors.

Supplemental document. See Supplement 1 for supporting content.

Biomedical Optics EXPRESS

References

1. A. Gabrielli, E. V. Avvedimento, and T. Krieg, "Scleroderma," N. Engl. J. Med. **360**(19), 1989–2003 (2009).
2. L. Zhong, M. Pope, Y. Shen, J. J. Hernandez, and L. Wu, "Prevalence and incidence of systemic sclerosis: A systematic review and meta-analysis," Int. J. Rheum. Dis. **22**(12), 2096–2107 (2019).
3. L. M. Calderon and J. E. Pope, "Sclerodersma epidemiology update," Curr. Opin. Rheumatol. **33**(2), 122–127 (2021).
4. V. D. Steen, "The many faces of scleroderma," Rheum. Dis. Clin. North Am. **34**(1), 1–15 (2008).
5. M. Kajii, C. Suzuki, J. Kashihara, F. Kobayashi, Y. Kubo, H. Miyamoto, T. Yuuki, T. Yamamoto, and T. Nakae, "Prevention of excessive collagen accumulation by human intravenous immunoglobulin treatment in a murine model of bleomycin-induced scleroderma," Clin. Exp. Immunol. **163**(2), 235–241 (2011).
6. W. Wu, S. Jordan, N. Graf, J. de Oliveira Pena, J. Curram, Y. Allanore, M. Matucci-Cerinic, J. E. Pope, C. P. Denton, D. Khanna, and O. Distler, "Progressive skin fibrosis is associated with a decline in lung function and worse survival in patients with diffuse cutaneous systemic sclerosis in the European Scleroderma Trials and Research (EUSTAR) cohort," Ann. Rheum. Dis. **78**(5), 648–656 (2019).
7. L. Shand, M. Lunt, S. Nihtyanova, M. Hoseini, A. Silman, C. M. Black, and C. P. Denton, "Relationship between change in skin score and disease outcome in diffuse cutaneous systemic sclerosis: application of a latent linear trajectory model," Arthritis Rheum. **56**(7), 2422–2431 (2007).
8. D. Khanna, D. E. Furst, P. J. Clements, Y. Allanore, M. Baron, L. Czirjak, O. Distler, I. Foeldvari, M. Kuwana, M. Matucci-Cerinic, M. Mayes, T. Medsger, P. A. Merkel, J. E. Pope, J. R. Seibold, V. Steen, W. Stevens, and C. P. Denton, "Standardization of the modified rodnan skin score for use in clinical trials of systemic sclerosis," J. Scleroderma Relat. Disord. **2**(1), 11–18 (2017).
9. R. Ionescu, S. Rednic, N. Damjanov, C. Varjú, Z. Nagy, T. Minier, L. Czirják, R. Ionescu, S. Rednic, N. Damjanov, C. Varjú, Z. Nagy, T. Minier, and L. Czirják, "Repeated teaching courses of the modified Rodnan skin score in systemic sclerosis," Clin. Exp. Rheumatol. **28**(2 Suppl 58), S37–S41 (2010).
10. M. Aringer, G. Riemekasten, and M. Matucci-cerinic, "The EUSTAR model for teaching and implementing the modified Rodnan skin score in systemic sclerosis," Ann. Rheum. Dis. **66**(7), 966–969 (2007).
11. M. Kaldas, P. P. Khanna, D. E. Furst, P. J. Clements, W. Kee Wong, J. R. Seibold, A. E. Postlethwaite, and D. Khanna, "Sensitivity to change of the modified Rodnan skin score in diffuse systemic sclerosis–assessment of individual body sites in two large randomized controlled trials," Rheumatology **48**(9), 1143–1146 (2009).
12. O. Kaloudi, F. Bandinelli, E. Filippucci, M. L. Conforti, S. Guiducci, F. Porta, A. Candelieri, D. Conforti, G. Grassiri, W. Grassi, and M. Matucci-cerinic, "High frequency ultrasound measurement of digital dermal thickness in systemic sclerosiss," Ann. Rheum. Dis. **69**(6), 1140–1143 (2010).
13. C.-H. Liu, S. Assassi, S. Theodore, C. Smith, S. Aglyamov, C. Mohan, and K. V. Larin, "Translational optical coherence elastography for assessment of systemic sclerosis," J. Biophotonics **12**(12), e20190023 (2019).
14. G. Abignano, S. Z. Aydin, C. Castillo-gallego, V. Liakouli, D. Woods, A. Meekings, R. J. Wake, D. G. Mcgonagle, P. Emery, and F. D. Galdo, "Virtual skin biopsy by optical coherence tomography : the first quantitative imaging biomarker for scleroderma," Ann. Rheum. Dis. **72**(11), 1845–1851 (2013).
15. P. A. Merkel, N. P. Silliman, C. P. Denton, D. E. Furst, D. Khanna, P. Emery, V. M. Hsu, J. B. Streisand, R. P. Polisson, A. Åkesson, J. Coppock, F. Hoogen, and A. Herrick, "Validity, Reliability, and Feasibility of Durometer Measurements of Scleroderma Skin Disease in a Multicenter Treatment Trial," Arthritis Rheum. **59**(5), 699–705 (2008).
16. D. J. Cuccia, F. P. Bevilacqua, A. J. Durkin, F. R. Ayers, and B. J. Tromberg, "Quantitation and mapping of tissue optical properties using modulated imaging," J. Biomed. Opt. **14**(2), 024012 (2023).
17. A. Mazhar, S. A. Sharif, J. D. Cuccia, J. S. Nelson, K. M. Kelly, and A. J. Durkin, "Spatial Frequency Domain Imaging of Port Wine Stain Biochemical Composition in Response to Laser Therapy : A Pilot Study," Lasers Surg. Med. **44**(8), 611–621 (2012).
18. S. A. Sharif, E. Taydas, A. Mazhar, R. Rahimian, K. M. Kelly, B. Choi, and A. J. Durkin, "Noninvasive clinical assessment of port-wine stain birthmarks using current and future optical imaging technology: a review," Br. J. Dermatol. **167**(6), 1215–1223 (2012).
19. F. R. Ayers, D. J. Cuccia, K. M. Kelly, and A. J. Durkin, "Wide-field spatial mapping of in vivo tattoo skin optical properties using modulated imaging," Lasers Surg. Med. **41**(6), 442–453 (2009).
20. R. B. Saager, A. N. Dang, S. S. Huang, K. M. Kelly, and A. J. Durkin, "Portable (handheld) clinical device for quantitative spectroscopy of skin, utilizing spatial frequency domain reflectance techniques," Rev. Sci. Instrum. **88**(9), 094302 (2017).
21. D. J. Cuccia, F. Bevilacqua, A. J. Durkin, and B. J. Tromberg, "Modulated imaging : quantitative analysis and tomography of turbid media in the spatial-frequency domain," Opt. Lett. **30**(11), 1354–1356 (2005).
22. S. Tabassum, Y. Zhao, R. Istfan, J. Wu, D. J. Waxman, and D. Roblyer, "Feasibility of spatial frequency domain imaging (SFDI) for optically characterizing a preclinical oncology model," Biomed. Opt. Express **7**(10), 4154–4170 (2016).
23. Y. Zhao, S. Tabassum, S. Piracha, M. S. Nandhu, M. Viapiano, and D. Roblyer, "Angle correction for small animal tumor imaging with spatial frequency domain imaging (SFDI)," Biomed. Opt. Express **7**(6), 2373–2384 (2016).
24. E. Y. Kissin, P. A. Merkel, and R. Lafyatis, "Myofibroblasts and hyalinized collagen as markers of skin disease in systemic sclerosis," Arthritis Rheum. **54**(11), 3655–3660 (2006).

Biomedical Optics EXPRESS

25. P. A. Merkel, P. J. Clements, J. D. Reveille, M. E. Suarez-Almazor, G. Valentini, and D. E. Furst, "Current status of outcome measure development for clinical trials in systemic sclerosis. Report from OMERACT 6," J. Rheumatol. **30**(7), 1630–1647 (2003).
26. L. Li, L. Zeng, Z. J. Lin, M. Cazzell, and H. Liu, "Tutorial on use of intraclass correlation coefficients for assessing intertest reliability and its application in functional near-infrared spectroscopy–based brain imaging," J. Biomed. Opt. **20**(5), 050801 (2015).
27. M. J. Bland and D. Altman, "Statistical methods for assessing agreement between two methods of clinical measurement," Lancet **1**(8476), 307–310 (1986).
28. N. Kollias and A. Baqer, "Spectroscopic Characteristics of Human Melanin In Vivo," J. Invest. Dermatol. **85**(1), 38–42 (1985).
29. T. Phan, R. Rowland, A. Ponticorvo, B. C. Le, R. H. Wilson, S. A. Sharif, G. T. Kennedy, N. P. Bernal, and A. J. Durkin, "Characterizing reduced scattering coefficient of normal human skin across different anatomic locations and Fitzpatrick skin types using spatial frequency domain imagings," J. Biomed. Opt. **26**(2), 026001 (2021).
30. A. P. Sappino, I. Masouyé, J. H. Saurat, and G. Gabbiani, "Smooth muscle differentiation in scleroderma fibroblastic cells," Am. J. Pathol. **137**(3), 585–591 (1990).
31. M. J. Hicks and C. Mohan, "Rapid, noninvasive quantitation of skin disease in systemic sclerosis using optical coherence elastography," J. Biomed. Opt. **21**(4), 46002 (2016).
32. C. K. Hayakawa, K. Karrobi, V. E. Pera, D. M. Roblyer, and V. Venugopalan, "Optical sampling depth in the spatial frequency domain," J. Biomed. Opt. **24**(07), 1–14 (2018).
33. K. Karrobi, A. Tank, S. Tabassum, V. Pera, and D. Roblyer, "Diffuse and nonlinear imaging of multiscale vascular parameters for in vivo monitoring of preclinical mammary tumors," J. Biophotonics **12**(6), e201800379 (2019).
34. S. Tabassum, A. Tank, F. Wang, K. Karrobi, C. Vergato, I. J. Bigio, D. J. Waxman, and D. Roblyer, "Optical scattering as an early marker of apoptosis during chemotherapy and antiangiogenic therapy in murine models of prostate and breast cancer," Neoplasia **23**(3), 294–303 (2021).
35. D. M. McClatchy, E. J. Rizzo, W. A. Wells, P. P. Cheney, J. C. Hwang, K. D. Paulsen, B. W. Pogue, and S. C. Kanick, "Wide-field quantitative imaging of tissue microstructure using sub-diffuse spatial frequency domain imaging," Optica **3**(6), 613–621 (2016).
36. J. Leppink, K. Winston, and P. O'Sullivan, "Statistical significance does not imply a real effect," Perspect Med. Educ. **5**(2), 122–124 (2016).